Science of Sintering, **50** (2018) 347-355

doi: https://doi.org/10.2298/SOS1803347L

UDK 535.37; 532.74

Effect of Eu^{3+} - Dopant Concentration on Structural and Luminescence Properties of Sry_2o_4 Nanocrystalline Phosphor and Potential Application in Dye-Sensitized Solar Cells

Vesna Lojpur[1*)], Stevan Stojadinović[2], Miodrag Mitrić[1]

[1]University of Belgrade, Vinca Institute of Nuclear Sciences, P.O. Box 522, 11001 Belgrade, Serbia

[2]Faculty of Physics, University of Belgrade, Studentski trg 12–16, 11000 Belgrade, Serbia

Abstract:

SrY_2O_4 phosphors were doped with different concentrations of Eu^{3+} (0.5, 1, 2, 4, 8 and 10 at %) in order to investigate the maximal doping concentration of Eu^{3+} and its implementation in solar cell devices. Samples were synthesized by a combustion method using citric acid and glycine as a fuel. The X-ray diffraction (XRD) patterns confirmed pure phase of SrY_2O_4. FE-SEM micrographs showed agglomerate phenomenon with spherical-like shape particles and diameter of about 50 nm. Upon excitation with 280 nm, emission spectra were recorded in the range from 450-750 nm and in all samples the same energy transitions were observed $^5D_0 \rightarrow {}^7F_J$ (J = 1, 2, 3 and 4) with maximal intensity for sample with 8 at % of Eu^{3+}. That sample was further examined for the purpose of application in solar cell devices and showed high value of efficiency at low light intensities.

***Keywords**: Luminescence; Phosphors; SrY_2O_4; Hypericin; Solar cells.*

1. Introduction

In a last couple of decades, phosphors are indispensable materials for applications in solid state lighting, especially in the form of light emitting diodes (LEDs) [1, 2]. Phosphors doped with rare earth ions give rise to strong emissions and plays important role in modern display technology, such as plasma display panel (PDP), white light emitting diodes (WLEDs), field emission display (FED) and in industry lighting, such as tricolor lamps and solar cells [3-7]. On the other hand, dye-sensitized solar cells (DSSCs) attracted a lot of attention due to the low fabrication cost and high efficiency [8-10]. The biggest challenge in DSSCs is chemical stability as well as conversion efficiency. One of the manners for reducing the energy losses is using of luminescent materials (down-conversion, up-conversion, down-shifting) that could modify the solar energy spectrum. Accordingly, it is always a challenge to find new materials that can respond to the ever-changing challenges posed by modern technology.

In previous years, a lot of phosphors with various host materials was synthesized and explored, which in themselves contained ions of rare-earth or transition metal. Binary rare-earth oxide phosphors are well known for its chemical and temperature stability, high luminescence efficiency and so on [11-17]. Among them sesquioxides (RE_2O_3, RE = rare earth) were investigated the most, but along with them there is another significant group of oxides with the formula ARE_2O_4 (A= Ca, Ba, Sr). This group of materials possesses excellent photoluminescence and magnetic properties which makes them very interesting for research

*) **Corresponding author:** lojpur@vinca.rs

[18, 19].

The SrY_2O_4 lattice belongs to the $CaFe_2O_4$ related structure consisting of one strontium and two yttrium sites, both of inversion symmetry. It is usually doped with Ce^{3+}, Eu^{3+}, Dy^{3+} and Sm^{3+} for down-conversion luminescence, with Yb^{3+}/ Er^{3+} for up-conversion as well as doped with Tb^{3+}/Tm^{3+}/Dy^{3+} for producing white light [20-23]. Rare earth ions shows abundant emission color based on their 4f→4f or 4f→5d transitions.

The SrY_2O_4 doped with Eu^{3+} is known as a promising down-conversion red phosphor since it give rise to strong emission at approximately 610 nm. At first, this material was produced using solid state reaction [24]. However, when SrY_2O_4 noteworthy the scientific attention because of his favorable characteristic, material was produced by other soft chemical methods. In that way, temperature of preparation of material was reduced as well as particle size with improvement of luminescence properties. Dubey et al., obtained SrY_2O_4 doped with Eu^{3+} by solid state reaction at 1400 °C [25]. Characterization of material showed that Eu^{3+} ion is accommodating in 2 non-equivalent sites of Y^{3+} and one site of Sr^{2+}. Zhou et al synthesized the same material by sol-gel method (using citric acid and polyethylene glycol) at significantly lower temperature (1000 °C) and reveal occupation of two sites of Y^{3+} by Eu^{3+} ions [26]. In addition, the best luminescent characteristics were obtained when doping concentration was 2 at%. So-Jung Park et al. prepared SrY_2O_4: Eu^{3+} *via* combustion synthesis also at 1000 °C and confirmed preferential accommodation Eu^{3+} in Y^{3+} sites [27].

In this paper, we prepared SrY_2O_4: Eu^{3+} with various concentrations of Eu^{3+} (from 0.5 to 10 at %) by combustion method using citric acid and glycine. We examined phase composition and microstructural parameters, morphology, as well as dependence of Eu^{3+}concentration on photoluminescent properties. Also, we used the best sample for preparation of dye-sensitized solar cell and investigated it efficiency.

2. Experimental Section

2.1. Materials

Starting materials for obtaining Eu^{3+} doped SrY_2O_4 were rare earth nitrates, yttrium nitrate hexahidrate ($Y(NO_3)_3{\cdot}6H_2O$) and europium nitrate hexahidrate ($Eu(NO_3)_3{\cdot}6H_2O$, Alfa Aesar (purity 99.9 %) and strontium nitrate $Sr(NO_3)_2$ also purchesed from Alfa Aesar (99 %). Glycine and citic acid was product of Acros (99+% and 99.6%, respectively). Indium tin oxide (ITO) ($In_2O_3(SnO_2)_x$)) coated glass (75×25×1.1 mm) were obtained from Sigma-Aldrich. Aluminum foil (15-μm thickness) (Purity > 99.3 %) were bought from MTI Korea. All chemicals were analytical grade reagents and were used directly without further purification.

2.2. Synthesis method

Samples of SrY_2O_4 nanocrystalline phosphors doped with different concentration of Eu^{3+} (0.5, 0.5, 1, 2, 4, 8 and 10 at %) were prepared *via* combustion synthesis using citric acid and glycine as fuel. Rare earth nitrates (solution 1) as well as strontium nitrate (solution 2) were dissolved in deionized water. Then citric acid was added in both solutions separately and left for dissolving for a half an hour heated on a hot plate at 60 °C with continued magnetic stirring. Afterwards, the solutions were emerged, glycine was added and temperature was lifted at 120 °C. After approximately one hour solution evaporated, wet gel was produced and subsequently burned in the furnace at 500 °C for 1.5 h. Finally, sample was additionally thermally treated for 2 h at 1000 °C. The same procedure was used for preparation of all samples. The extraction of St. John's wort was carried out with ethanol to obtain valuable components and neutral agents rich was extracted.

2.3. Fabrication of solar cell device

The solar cell consisted of composite SrY_2O_4 doped with 8 at% Eu^{3+} and dye (hypericin) and it is dispersed on ITO-coated glass as a working electrode, aluminium as a counter electrode and PVA matrix as a solid carrier of electrolyte (0.5M KI+ 0.05M I_2). Hypericin was previously extracted in ethanol from the St. John's wort and together with the SrY_2O_4 doped with 8 at% Eu^{3+} used for deposition of the thin layer. For the layer thickness of 100 nm, 5 mg of powder was dispersed in 2 ml hypericin solution. The film was dispersed by spraying (hand-made) on pre-heated ITO glass at the temperature of 80 °C and subsequently dried at 100 °C in an oven for 24h.

2.4. PVA matrix membrane synthesis

Radiolytic synthesis of 5 % (w/w) PVA matrix includes: preparation of PVA solution, gamma irradiation, post irradiation treatment and immersion obtained hydrogel in electrolyte solution. PVA solution was obtained by dissolving PVA in deionized water at 90 °C under the constant stirring for 6 hours. After that, the solution was saturated with Ar, poured in the glass mold and gamma irradiated in the 60 Co radiation facility. Irradiation was performed at room temperature at a dose rate of 0.52 kGy/h up to the integral radiation dose of 25 kGy. Cross-linked hydrogel eas obtained in the swollen state and immersed in the electrolyte solution.

2.5. Characterization

The structure analysis of SrY_2O_4 phosphors doped with x at % Eu^{3+} was checked by XRD measurement using Philips PW-1050 with CuK_α radiation. The patterns were recorded in the 2θ range from 20 to 70° with a fixed 1° divergence and 0.1° receiving slit. Schematic representation of SrY_2O_4 structure is drawn in Vesta program. Particle size and morphology ware estimated from FE-SEM micrographs (FEI Scios 2, operating voltage of 30 kV). Chemical compositions of samples were estimated by energy dispersive X-ray spectroscopy (EDS). Photoluminescent properties PL spectral measurements were taken on a Horiba Jobin Yvon Fluorolog FL3-22 spectrofluorometer at room temperature, with a Xe lamp as the excitation light source. The obtained spectra were corrected for the spectral response of the measuring system and spectral distribution of the Xe lamp. Current-voltage (*I-V* curve) characteristics of the cells were measured under 50 and 350 W/m^2 (5 % and 35 % sun), illumination using Philips ELH 120V 300W lamp. Current-voltage characteristics were registered with a Keithley 237 Sourcemeter (V-I sweep mode, range 0 V - V_{OC}, variable voltage step, delay time of 0.040 s). The illumination intensity was calibrated with a referent monocrystalline silicon cell.

3. Results and discussion

3.1. X-ray diffraction (XRD) analysis

Crystal structures of synthesized samples were determined by X-ray powder diffraction. XRD patterns are indexed with the card PDF No. 01-074-0264, and one representative diffractogram is presented in Fig.1. Crystallite size is calculated by using Scherrer formula:

$$d = \frac{K \cdot \lambda}{\beta \cdot \cos\theta} \quad (1)$$

where *d* is the mean size of the ordered (crystalline) domains, K is a dimensionless shape factor, with a value close to unity. The shape factor has a typical value of about 0.9, but varies (0.9-1) with the actual shape of the crystallite, λ is the X-ray wavelength, β is the line broadening at half the maximum intensity (FWHM) and θ is the Bragg angle. Values for crystallite size were the following: 36.42 nm for sample with 0.5at % Eu^{3+}, 38.78 m for 1 at % Eu^{3+}, 41.07 nm for 2 at % Eu^{3+}, 44.13 nm for 4 at% Eu^{3+}, 46.62 nm for 8 at % Eu^{3+} and 53.20 nm for sample with 10 at % Eu^{3+}. It is obvious that with increasing of doping concentration, crystallite size is becoming bigger. Taking into account that Eu^{3+} ion (0.95 Å) is greater than Y ion (0.89 Å), enhancement of cell parameter is a logical consequence and therefore also affects crystallite size. SrY_2O_4 crystallizes into an orthogonal structure with space group Pnam (62). The Sr atoms are coordinated by eight oxygens and the Y atoms by six oxygens (Fig. 2). Y^{3+} ions have two non-equivalent sites with C_s symmetry. The Y_1 site is nearly octahedral while the Y_2 site is a little distorted.

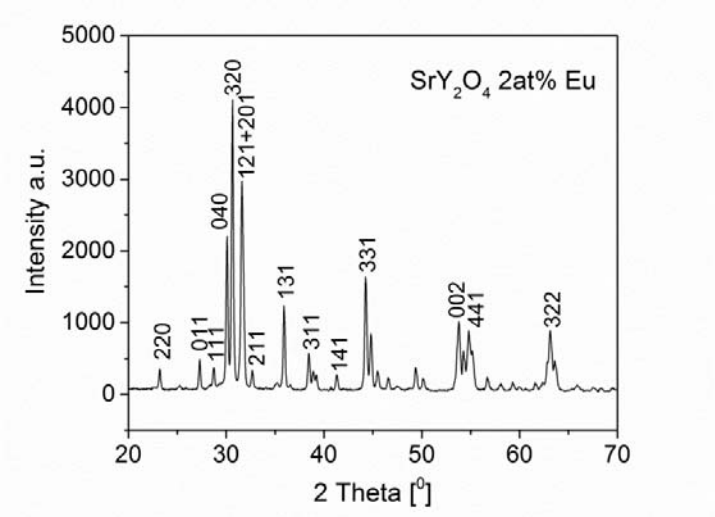

Fig. 1. Representative XRD diffractogram for SrY_2O_4 doped with 2 at% of Eu^{3+}.

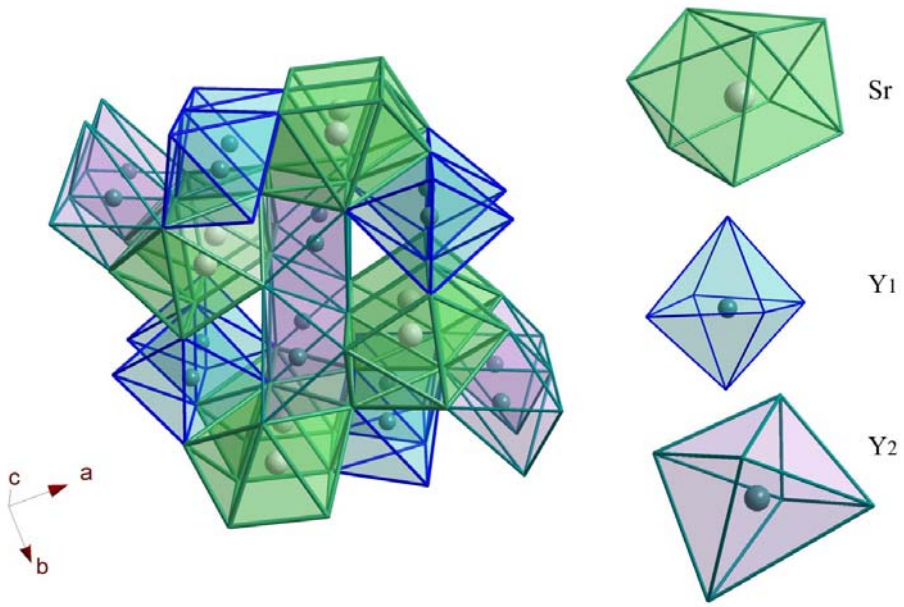

Fig. 2. Schematic representation of SrY_2O_4 crystal structure along with the coordination environment of the Sr and Y_1 and Y_2 sites in SrY_2O_4.

3.2. FE-SEM and EDS analysis

FE-SEM and EDS analysis was carried out to investigate the morphology and chemical characterization, respectively. One representative sample of SrY_2O_4 doped with 2 at % Eu^{3+} is presented in Fig. 3. FE-SEM observation revealed that at micron level, powders consist of porous agglomerated particles. Pores are a consequence that comes from the large quantity of gases developing during this type of synthesis method. It can be clearly seen that agglomerated particles are caused by sticking spherical particles with size of about 50 nm. The EDS analysis confirmed existence of elements that are present in the structure. During this measurement the accumulation was low, with not enough counts to register presence of Eu. Due to that, Eu isn't mark because it is in noise level.

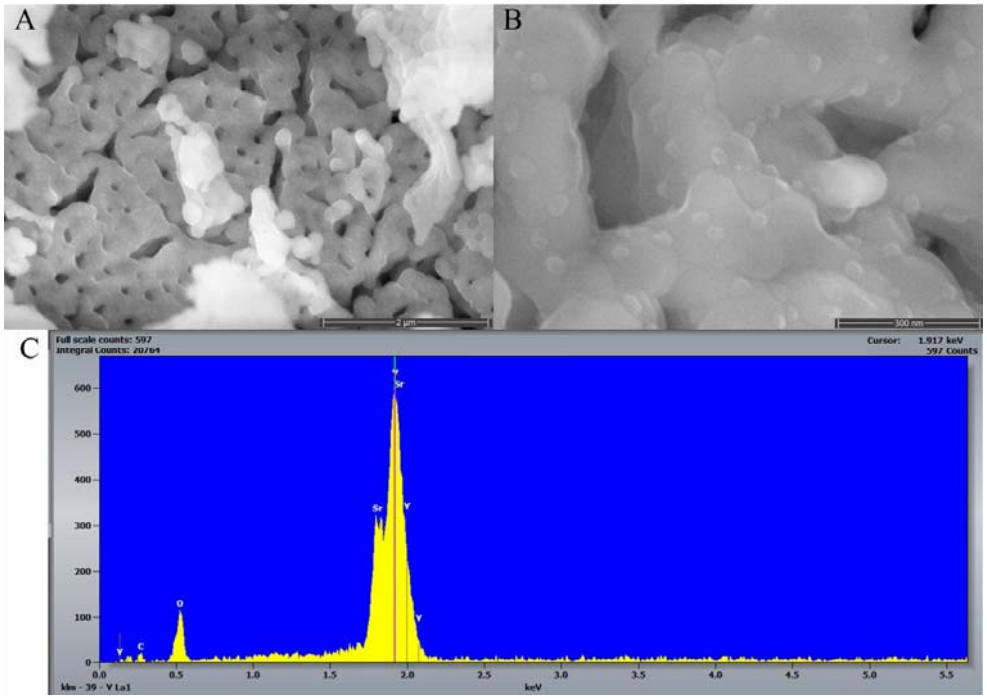

Fig. 3. FE-SEM micrographs of the sample SrY_2O_4: 2at% Eu^{3+} (A magnification 35.000 and B magnification 200.000) and EDS (C).

3.3. Photoluminescent properties

One randomly selected excitation spectrum recorded with emission at 614 nm for the sample with 0.5 at % Eu^{3+} is presented in Fig. 4. It is obvious that the strongest peak is positioned at 280 nm and hence that was the excitation wavelength used for measuring the emission spectra.

Emission spectra for SrY_2O_4: x at % Eu (x= 0.5, 1, 2, 4, 8, and 10) recorded in room temperature under the same experimental conditions in the range from 450 to 750 nm, are presented in Fig. 5. Upon excitation with 280 nm in all samples the same energy transitions were observed $^5D_0 \rightarrow {}^7F_J$ (J= 1, 2, 3 and 4). Transition $^5D_0 \rightarrow {}^7F_1$ is in the 574 - 602 nm range with maximum at 590 nm, $^5D_0 \rightarrow {}^7F_2$ in 605-635 nm range with maximum at 614 nm, $^5D_0 \rightarrow {}^7F_3$ is 643-667 nm range with maximum at 651nm, and $^5D_0 \rightarrow {}^7F_4$ is in the 680-718 nm range with maximum at 706 nm in the photoluminescent spectrum. As it was previously said in the structure section, there are two non-equivalent sites of Y^{3+} ions for substitution with Eu^{3+} ion. Accommodation of Eu^{3+} ion in Sr^{2+} site is more complicated due to the large ionic mismatch

(Sr^{2+} 1.13 Å) and different valence state requiring in addition high temperatures above 1400 °C. With increasing of dopant concentration, intensity of emission increases until 8 at % of Eu^{3+} (see green line in Fig. 4) and after that starts to decrease when doping concentration was 10 at %.

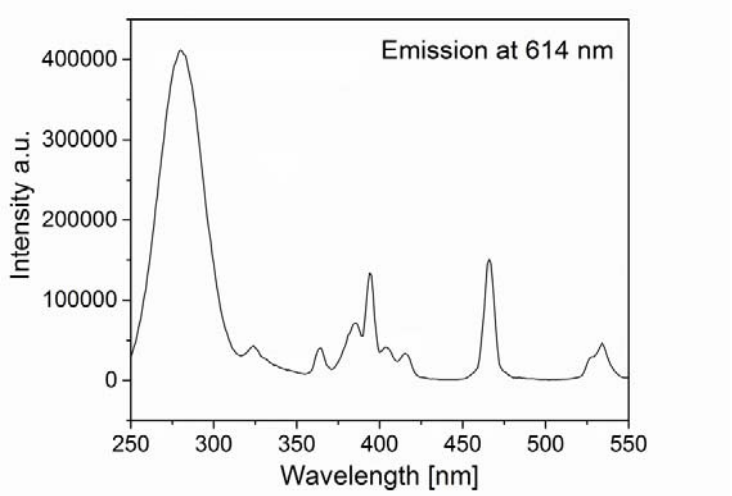

Fig. 4. Excitation spectrum for SrY_2O_4:0.5 at % Eu recorder with emisson at 614 nm.

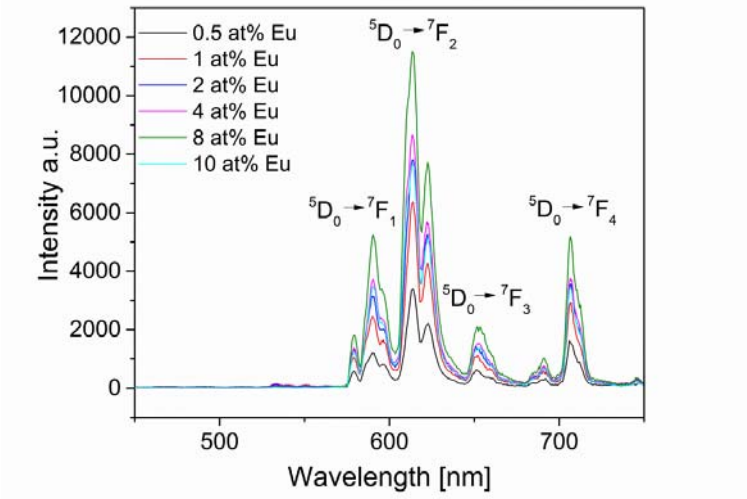

Fig. 5. Emission spectra for SrY_2O_4: x at % Eu (x= 0.5, 1, 2, 4, 8 and 10) with characteristic transitions excited at 280 nm.

3.4. Application in solar cells

Designed solar cell was made using a natural dye hypericin and sample that showed the highest luminescent intensity, which was SrY_2O_4: 8 at % Eu. Preparation of the solar cell was explained in experimental section while its schematic representation is given in Fig. 6.

Typical illuminated *I-V* plots of fabricated solar cells under the low (5 % sun) and medium (35 % sun) illumination are shown in Fig. 6. Two cells (A and B) are made to be the same. The efficiency □ was calculated from the well-known relation □ = V_{oc}*I_{sc}*FF/P_{input}*100, where P_{input} is the input light energy. The fill factors (FF) were calculated from the relation FF = I_m*V_m/I_{sc}*V_{oc}, where I_m and V_m are the maximum current and voltage , and I_{sc} and V_{oc} are the short circuit current and the open-circuit voltage, respectively. Whole cell surface was 7.5 cm^2, while illuminated part was 3 cm^2.

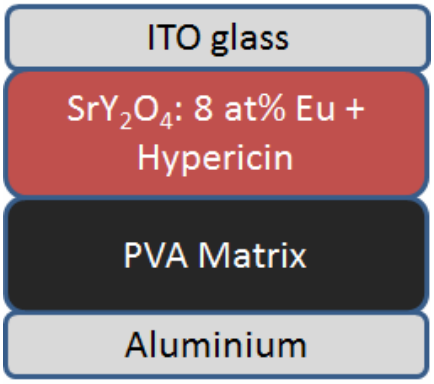

Fig. 6. Schematic representation of designed solar cell.

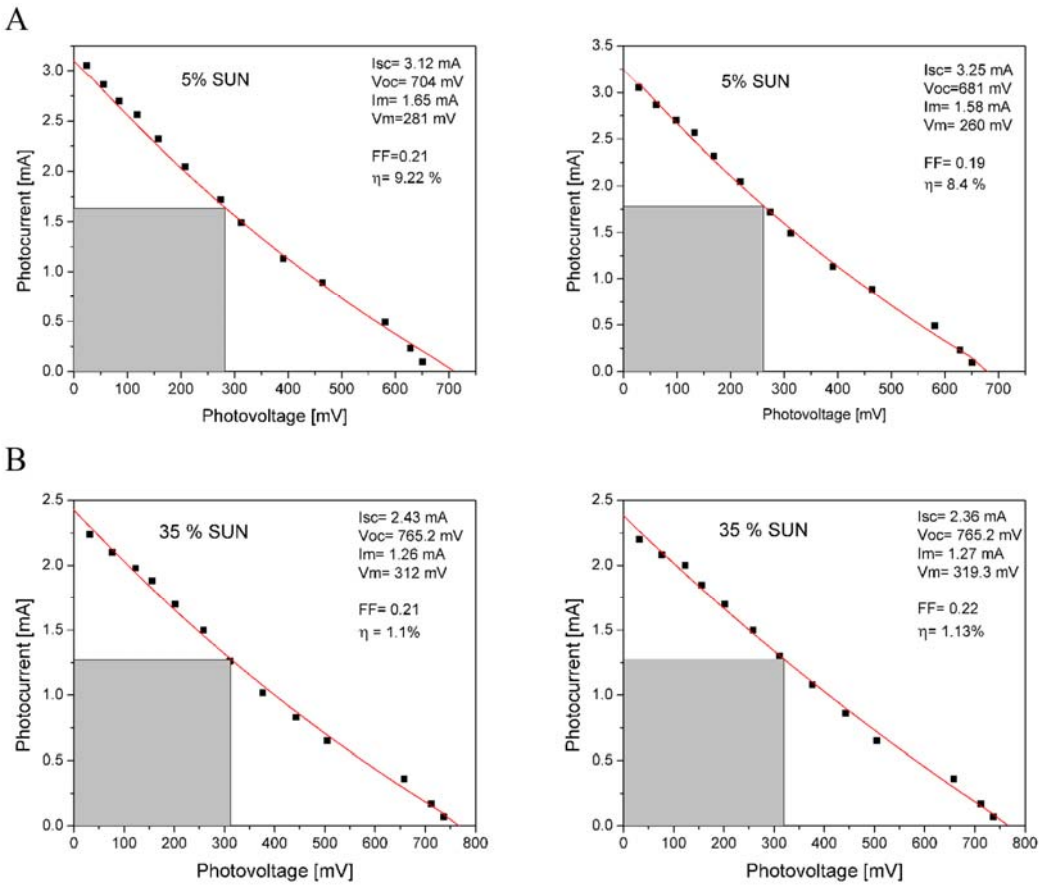

Fig. 7. Illuminated I-V curves for the same two solar cells made of ITO/composite SrY_2O_4:8 at% Eu^{3+} and hypericin/aluminium.

For the illumination of 5 % sun obtained results of efficiency was around 9 %, while for 35 % sun the efficiency was 1 % (calculated for the entire cell area). The shapes of *I-V* curves are inverse exponential so the FF is below 0.25 (value for linear dependence). Series (Rs) and shunt (Rsh) resistances plays important role on the shape of the illuminated I-V curves. Reasons for this behaviour is existance of an extra resistance in the cell. In case of inverse exponential curve the values of series resistance are higher than the values of shunt

resistances. The PVA matrix is not conductive and serves only as a carrier of elecrolyte. In that way, introduction of PVA in the construction of solar cell reduces the mobility of the electons which represents an additional resistance in the solar cell.

4. Conclusion

Having all discussed results in consideration, it can be concluded that with presented synthesis method pure and nanocrystalline SrY_2O_4: x at % Eu samples were obtained. Structural analysis as well as photoluminescent measurements confirmed efficient accommodation of Eu^{3+} in two non-equivalent sites of Y^{3+}. Combustion synthesis provided obtaining samples with crystallite size of around 30 nm and particle size of about 50 nm. This synthesis also enabled the highest concentration dopant of 8 at % Eu^{3+} which is considerably higher than other methods of synthesis. Use of this sample in dye-sensitized solar cells provides very good efficiency, 9 % for illumination of 5 % sun, and 1 % for the illumination of 35 % sun. These results imply that luminescent material SrY_2O_4 doped with Eu^{3+} can be used in solar cell applications.

Acknowledgments

This work is supported by the Ministry of Education, Science and Technological Development of the Republic of Serbia (grants No. 45005) and Program Start up for science.

5. Reference

1. J. Zhang, M. Chen, Y. Gao, Displays, 49 (2017) 35.
2. V. Kumar, M. Manhas, A.K. Bedyal, H.C. Swart, Mater. Res. Bull. 91 (2017) 140.
3. J. T. Ingle, R.P. Sonekar. S.K. Omanwar, Y. Wang, L. Zhao, J. Alloy. Compd., 608 (2014) 235.
4. T. Senden, E. J. van Harten, A. Meijerink, J. Lumin., Article in Press https://doi.org/10.1016/j.jlumin.2017.10.006
5. Q. Wu, J. Ding, Y. Li, X. Wang, Y. Wang, J. Amer. Ceram. Soc., 100 (2017) 3088.
6. Y. Liu, D. Wang, Optoelectron Lett., 1 (2010) 34.
7. A. Bouajaj, S. Bolmokhtar, M.R. Britel, C. Armellini, B. Boulard, F. Belluomo, A. Di Stefano, S. Polizzi, A. Lukowiak, M. Ferrari, F. Enrichi, Opt. Mater., 52 (2016) 62.
8. M. N. Mustafa, S. Shafie, Z. Zainal, Y. Sulaiman, Material & Design, 136 (2017) 249.
9. M. Asemi, M. Ghanaatshoar, J. Amer. Ceram. Soc.,100 (2017) 5584.
10. T. Wan, S. Ramakrishna, Y. Liu, J. Appl. Polymer Sci., 135 (2018) 45649.
11. M. M. Medić, M. G. Brik, G. Dražić, Ž. M. Antić, V. M. Lojpur, M. D. Dramićanin, J. Phys. Chem. C, 119 (2015) 724.
12. V. Lojpur, M. G. Nikolić, D. Jovanović, M. Medić, Ž. Antić, M. D. Dramićanin, Appl. Phys. Lett. 103 (2013) 141912.
13. H. Jun, S.-H. Kim, S. Park, Opt. Mater., 72 (2017) 571.
14. M. Kaur, D. P. Bisen, N. Brahme, P. Singh, I.P. Sahu, Luminescence, 31 (2016) 728.
15. T. Pang, W.-H. Lu, Ceram. Int., 43 (2017) 1061.
16. R. Salhi, J.-L. Deschanvres, J. Lumin., 170 (2016) 231.
17. T. V. Gavrilović, D. J. Jovanović, V. Lojpur, A. Nikolić, M. D. Dramićanin, Sci. Sint. 47 (2015) 221.
18. T. Maekawa, K. Kurosaki, S. Yamanaka, Mat. Lett., 61 (2007) 2303.

19. V. Dubey, R. Tiwari, R. Shrivastava, C. Markande, O. Verma, J. K. Saluja, Y. Parganiha, K. V. R. Murthy, J. Disp. Technol., 12 (2016) 171.
20. J. Philippen, C. Guguschev, D. Klimm, J. Cryst. Growth, 459 (2017) 17.
21. E. Pavitra, G. S. R. Raju, J. S.Yu, J. Alloy. Compd., 592 (2014) 157.
22. Z. Fu, S. Zhou, Y. Yu, S. Zhang, J. Phyc. Chem. C, 109 (2005) 23320.
23. J. Yang, S. Xiao, J. Ding, X. Yang, X. Wang, J. Alloy. Compd., 474 (2009) 424.
24. X. Shen, M. Xing, Y. Tian, Y. Fu, Y. Peng, X. Luo, J. Rare Earth., 34 (2016) 458.
25. V. Dubey, J. Kaur, Y. Parganiha, N.S. Suryanarayana, K.V.R. Murthy, Appl. Radiat. Isot., 110 (2016) 16.
26. L. Zhou, J. Shi, M. Gong, J. Lumin., 113 (2005) 285.
27. S. J. Park, C. H. Park, B. Y. Yu, H.S. Bae, C. H. Kim, C.H. Pyun, J. Electrochem. Soc., 146 (1999) 3903.

Садржај: *SrY_2O_4 је допиран са различитим концентрацијама Eu^{3+} (0.5, 1, 2, 4, 8 and 10 at %) у циљу одређивања максималне концентрације допирања овог система са јонима Eu^{3+} као и примену овог материјала у соларним ћелијама. Узорци су синтетисани методом сагоревања користећи лимунску киселину и глицин као гориво. Рендгенска дифракција (XRD) је потврдила добијање чисте фазе SrY_2O_4. Скенирајући електронски микроскоп је показао да је узорак агломерисан са сферичним честицама пречника око 50 нм. Емисиони спектри су снимани у опсегу од 450-750 нм при ексцитацији на 280 нм и у свим узорцима су снимљени исти енергетскипрелази $^5D_0 \rightarrow {}^7F_J$ (J = 1, 2, 3 and 4) са максималним интезитетом за узорак са 8 at % Eu^{3+}. Таj узорак је даље испитиван у сврху примене у соларним ћелијама и показао је високу вредност ефикасности на ниским интезитетима светлости.*

Кључне речи*: луминесценција, фосфори, SrY_2O_4, цвекла, соларне ћелије.*